Effect of the properties of MFI zeolites on the esterification of isopentyl acetate

Maria E. Ribeiro (Investigation) (Formal analysis) (Writing - review and editing), Karen N. Franke (Formal analysis) (Writing - review and editing), Patrícia M. Lima (Conceptualization) (Writing - review and editing), Dilson Cardoso (Conceptualization) (Supervision) (Writing - review and editing) (Funding acquisition)

PII: S0920-5861(20)30470-3

DOI: https://doi.org/10.1016/j.cattod.2020.07.010

Reference: CATTOD 13002

To appear in: *Catalysis Today*

Received Date: 4 March 2020

Revised Date: 7 June 2020

Accepted Date: 17 July 2020

Please cite this article as: Ribeiro ME, Franke KN, Lima PM, Cardoso D, Effect of the properties of MFI zeolites on the esterification of isopentyl acetate, *Catalysis Today* (2020), doi: https://doi.org/10.1016/j.cattod.2020.07.010

Effect of the properties of MFI zeolites on the esterification of isopentyl acetate

Maria E. Ribeiro, Karen N. Franke, Patrícia M. Lima, Dilson Cardoso*

Catalysis Laboratory - Department of Chemical Engineering,

Federal University of São Carlos, 13565-905, São Carlos, SP, Brazil

*Corresponding author: dilson@ufscar.br

Graphical abstract

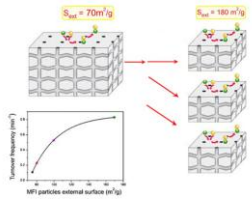

Highlights

- MFI zeolites with different aluminum contents were used to obtain isopentyl acetate
- Catalysts MFI with larger external surface obtained better catalytic performance
- The esterification over MFI occurs at the external surface of the particles
- The esterification reaction is limited by the internal diffusion

Abstract

Fusel oil is a by-product from the fermentation of sugar to produce ethanol. With the increase in ethanol production in the last years, thousands of liters of fusel oil are also generated. Thus, alternatives for reusing fusel oil involving the transformation of isopentanol, its main constituent, into products relevant to industry have aroused interest. In this work, the use of MFI zeolites with different contents of aluminum in the transformation of isopentyl into its ester, isopentyl acetate, was studied. Its main objective was to investigate the effects of the aluminum content of zeolites on textural and chemical properties and how they influence the

catalytic activity. In the work it was verified that the catalysts with larger external surface obtained better catalytic performance, suggesting that, due to the small pore diameter of the MFI structure, the reaction is limited by the effects of internal diffusion and occurs mainly at the external surface of the MFI particles.

Keywords: Esterification, MFI zeolite, shape selectivity, diffusional limitation, isopentyl acetate

1. Introduction

The alcohol industry generates several by-products and among these, fusel oil stands out, due to the high volume generated (65 million liters/year in Brazil) [1,2] and its composition, rich in higher alcohols such as isopentanol, isobutanol, butanol, and propanol [3,4]. Isopentanol is the main constituent of this by-product and can be used industrially to some products used in industry [3]. However, due to the high production, alternative uses of this by-product are essential to make the alcohol industries more profitable [4].

Esters are one of the main classes of organic compounds, used as flavorings in food, beverages, cosmetics and in the pharmaceutical industry [5]. Among the esters of isopentyl alcohol, isopentyl acetate stands out, one of the most used flavorings in the food industry with worldwide demand of approximately (74,000 kg/year), due to the strong aroma of fruits [1,6]. Furthermore, it can be used as a solvent, varnishes, silk, and films [7] .

Typically, esterification reactions can be performed using homogeneous acid catalysts, such as H_2SO_4 [8]. However, heterogeneous acid catalysts offer advantages in easing the separation of reaction products and the absence of equipment corrosion [9]. Thus, zeolites [8,10–12], ion exchange resins [7,8,13], sulfonated zirconia [8], niobium

oxides [8,14], among others, have been reported in the literature as potential catalysts for esterification reactions [9].

According to the literature, ion exchange resins were the first heterogeneous catalysts used in the esterification reaction of acetic acid with short-chain alcohols [8,13]. Although they have a high catalytic activity, resins have low thermal resistance, limiting their use to 120 °C and for short periods [8]. In addition to resins, niobium oxides have been shown to be efficient for esterification due to the high surface acidity [8,14]. Protonic zeolites such as Y, BEA and MFI also provide an interesting alternative in which the performance of these catalysts is based mainly on strong acidity due to the presence of Brønsted sites [8]. However, several parameters are mentioned in the literature that influences the catalytic performance of these materials, such as diffusional limitation in the pores, the type of channels (uni-bi and three-dimensional) and hydrophobicity [12].

In this work, acidic zeolites of MFI structure with different percentages of framework aluminum were applied as catalysts in the esterification of acetic acid to obtain isopentyl acetate. The objective is to investigate the effects of aluminum content on the textural, chemical and catalytic properties of zeolites.

2. Materials and methods

2.1. Preparation of catalysts

The ammoniacal zeolites with MFI structure (CBV 2314, CBV 3024E, CBV 2524G and CBV 8014) were purchased from Zeolyst International (USA). To obtain the protonated form, these materials were calcined in a muffle at a temperature of 500 ° C for 4 h, in a static atmosphere, using a heating ramp of 10 °C. min^{-1}.

The sodium zeolite MFI (SN-55) was acquired from ALSI-PENTA Zeolithe Gmbh and its acid form was achieved through ion exchange with aqueous NH_4Cl solution

(1 mol. L^{-1}). For this procedure, the sodium zeolite was subjected to three consecutive ion exchanges of 1 h; afterward, the material was washed with distilled water and dried at 80 °C for 24 h. After the ion exchange step, the material was calcined under the same conditions as the other ammoniacal samples. The nomenclature and some properties of the catalysts are shown in Table 1 and it shows almost all aluminum present in these zeolites are in the framework, as determined by ^{27}Al MAS-NMR [15].

Table 1. Nomenclature of commercial and acidic zeolites, their aluminum (% Al) and acidic sites content (N_{AS}).

Product Code	Si/Al	Catalyst Code[a]	% Al[b]	Al_f [c]	N_{AS} [d]
CBV 2314	11.5	HZ-8	7.7	nd	1.3
CBV 3024E	15	HZ-7	6.9	0.91	1.0
SN-55	22	HZ-5	5.4	nd	0.90
CBV 2524G	25	HZ-4	4.3	0.94	0.67
CBV 8014	40	HZ-3	2.5	0.97	0.41

[a]HZ= protonated zeolite.

[b] %Al= Molar fraction of aluminum estimated by EDS: 100*Al/ (Al+Si).

[c] Al_f= Framework aluminum molar fraction =Al_f/ (Al_f+Al_{ef}), [15].

[d] N_{AS} = acid sites mmols per catalyst gram.

EDS= Energy Dispersive X-Ray Spectroscopy.

nd = not determined

2.2. Characterizations

The confirmation of the structure of these zeolites was performed using a diffractometer (Miniflex 600, Rigaku) with Cu-Kα radiation (40 kV, 15 mA), varying 2θ in the range of 5 to 50 °.

The Si and Al content of the samples was determined by EDS; the samples were dispersed on double-sided carbon adhesive tapes and placed on sample holders. The analyses were performed in an XL FEG electron microscope, operated at a voltage of 20 kV.

The protonated catalysts were analyzed by scanning electron microscopy (SEM) to verify the shape and size of the particles. The sample suspensions were prepared by adding 20 mg of catalyst in methanol, performing the dispersion by means of ultrasound for 30 min. Subsequently, aliquots of the supernatant were dripped onto a sample holder until the deposition of the solid and complete evaporation of the solvent was observed. The micrographs were acquired by an XL FEG electron microscope, operated at a voltage of 5 kV.

The isotherms were carried out with a Micromeritics ASAP 2020 equipment. Initially, the samples were treated under vacuum, to eliminate physical water in the catalyst. After treatment, the volume of N_2 adsorbed at low pressures and at the boiling temperature of liquid nitrogen (-195.8 °C) was measured. The volume of micropores and the external surface area of the catalysts were calculated by analysis of nitrogen physisorption isotherms by the t-plot method.

The total amount of acidic sites in the zeolites was determined by ammonia desorption at programmed temperature (TPD-NH_3), using an AutoChem II 2920 chemisorption analyzer from Micromeritics.

2.3. Catalytic Tests

The catalytic activity of protonated zeolites was evaluated in the reaction of esterification of isopentanol with acetic acid whose mechanism is well known [7]. The esterification reaction was conducted in the proportion of acetic acid and isopentyl alcohol, as shown in Figure 1.

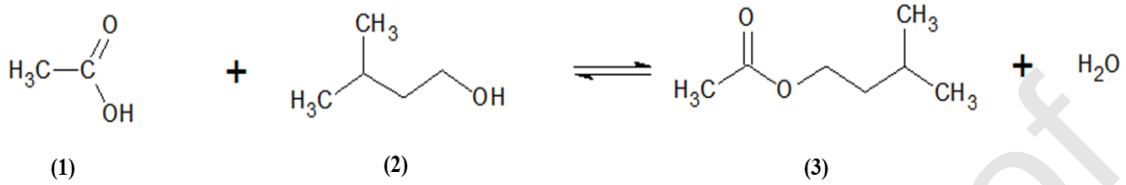

Figure 1. Scheme of the esterification between acetic acid and isopentanol.

The catalytic tests were carried out at 80 °C in a batch reactor equipped with a condenser. The initial reaction mixture (20 ml) contained equimolar amounts (0.12 mol) of the reagents (Sigma-Aldrich, 99%) and 4 wt% of catalyst in relation to mass of the reaction mixture. The reaction components were analyzed in a Shimadzu CG-2010 chromatograph containing an RTX-1 capillary column and a flame ionization detector (FID). In order to verify reproducibility, the catalytic tests were carried out in triplicate.

The conversion of acetic acid assumes that it is selectively consumed as shown in Figure 1, and was calculated using Equation 1, in which MA and MP are the number of moles of acetic acid and of the ester, respectively.

$$X_A(\%) = \frac{MP}{MA+MP} \times 100 \qquad \text{(Eq. 1)}$$

The kinetic curves obtained from the catalytic tests were adjusted by a hyperbolic model shown in Equation 2, where *t* is reaction time, *a* and *b* are specific parameters for each experimental reaction condition.

$$X_A = \frac{a.t}{(t+b)} \quad \text{(Eq. 2)}$$

The adjustment of the curves to this model allowed the determination of the conversion derivative of acetic acid at the beginning of the reaction, $dX_A/dt|_{t=0}$. This parameter allows to estimate the reaction rate at the initial moment of the reaction, $r_{A|t=0}$ by Equation 3, in which C_{A0} (mol. L^{-1}) is the initial concentration of acetic acid in the reaction mixture.

$$r_{A|t=0} = C_{A0} \ (dX_A/dt|_{t=0}) \quad \text{(Eq. 3)}$$

On the other hand, the turnover frequency at time zero, TOF_0 (min^{-1}), corresponds to the quotient between the reaction rate at the initial instant, $r_{A|t=0}$ (mol. L^{-1}. min^{-1}), and the number of mols of acidic sites present in the reaction medium N'_{AS} (mol H^+). TOF_0 can be calculated from Equation 4, where V(L) is the volume of the reaction mixture, N_{AS} (mol H^+. g^{-1}) is the number of acidic sites in a gram of catalyst and m_{cat} is the mass of catalyst in the reaction mixture.

$$TOF_0 = \frac{r_{A|t=0} \cdot V}{N'_{AS}} = \frac{C_{A0} \cdot V \cdot (dX_A/dt|_{t=0})}{N_{AS} \cdot m_{cat}} \quad \text{(Eq. 4)}$$

Finally, N_{AS} was calculated by Equation 5, based on the chemical composition of zeolite, where TCU (equal to 96) is the total number of silicon and aluminum tetrahedra in the unit cell. In this equation, x_{H^+} is equal to the molar fraction of aluminum in the zeolite network, Al_f (Table 1); MM_{H^+} is the molecular weight of H^+; $x_{(i)}$ represents the

molar fraction of Si or Al; $MM_{(i)}$ is the molecular mass of Si or Al; $MM_{(O2)}$ is the molecular mass of oxygen:

$$N_{AS} = \frac{TCU \,.\, x_{H^+} \,.\, MM_{H^+}}{\sum TCU \,.\, x_{(i)} \times MM_{(i)} + 2\, TCU \,.MM_{(O2)}} = \frac{x_{H^+} \,.\, MM_{H^+}}{\sum x_{(i)} . MM_{(i)} + 2 \,.\, MM_{(O2)}} \quad \text{(Eq. 5)}$$

Through equation 5, it was obtained that the N_{AS} of the catalysts HZ-8, HZ-7, HZ-5, HZ-4 and HZ-3 are 1.3, 1.1, 0.9, 0.67 and 0.41 mmol H^+/g of zeolite, respectively.

3. Results and Discussions

3.1. Characterization of catalysts

The result of the chemical analysis of zeolites in the protonic form is shown in Table 1. The aluminum content, % Al, of the zeolites determined by EDS is in accordance with the information reported by the manufacturers. The EDS technique showed that none of the samples presented Na^+ cations, revealing that the ion exchange achieved was 100% effective.

Figure 2 shows the X-ray diffractograms of the catalysts in the protonic form. All diffractograms showed the same profile with more intense peaks at 2θ angles located at 7.9; 8.9; 23.1 and 23.4 ° which are characteristic of zeolites with MFI structure according to the literature [16]. In addition, the presence of other zeolitic phases was not verified in the diffractograms.

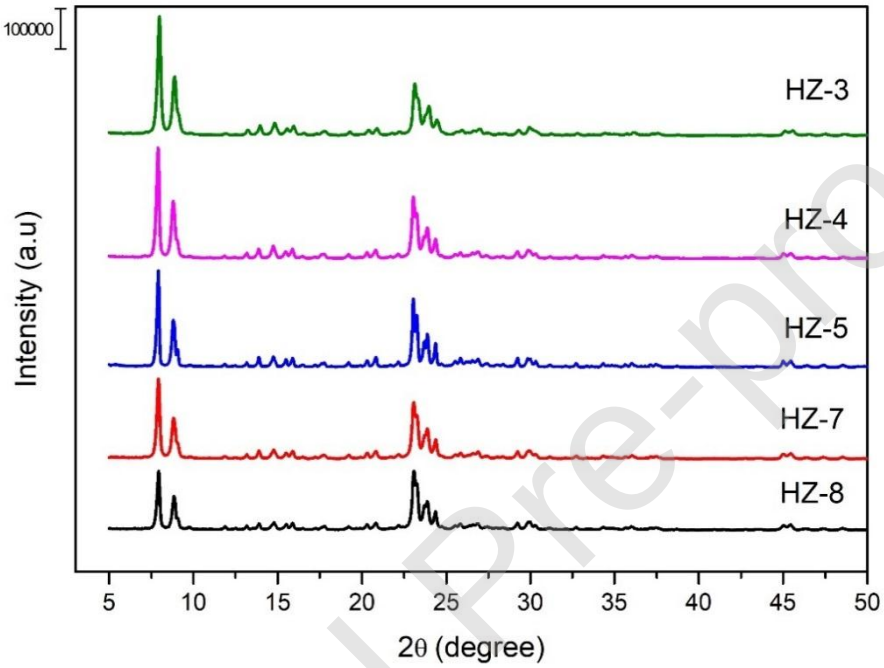

Figure 2. X-ray diffractograms of protonic zeolites with MFI structure.

The scanning electron microscopy images of the MFI catalysts with different aluminum contents are shown in Figure 3. The micrographs of the samples HZ-8, HZ-7, HZ-4 and HZ-3 (Fig. 3a, 3b, 3d, and 3e) revealed that they are formed by particles with irregular morphology and constituted by polycrystalline agglomerates with non-uniform size distribution. The micrograph of the HZ-5 zeolite (Fig. 3c), however, showed that it is formed by particles with well-defined morphology, in the form of hexagonal prisms, which is characteristic of the MFI materials [17]. In addition, it was found in Fig. 3c, that the HZ-5 particle size is much larger than the other samples. Other authors also found that the particle size and morphology of MFI materials depend on the aluminum content present in the structure [18].

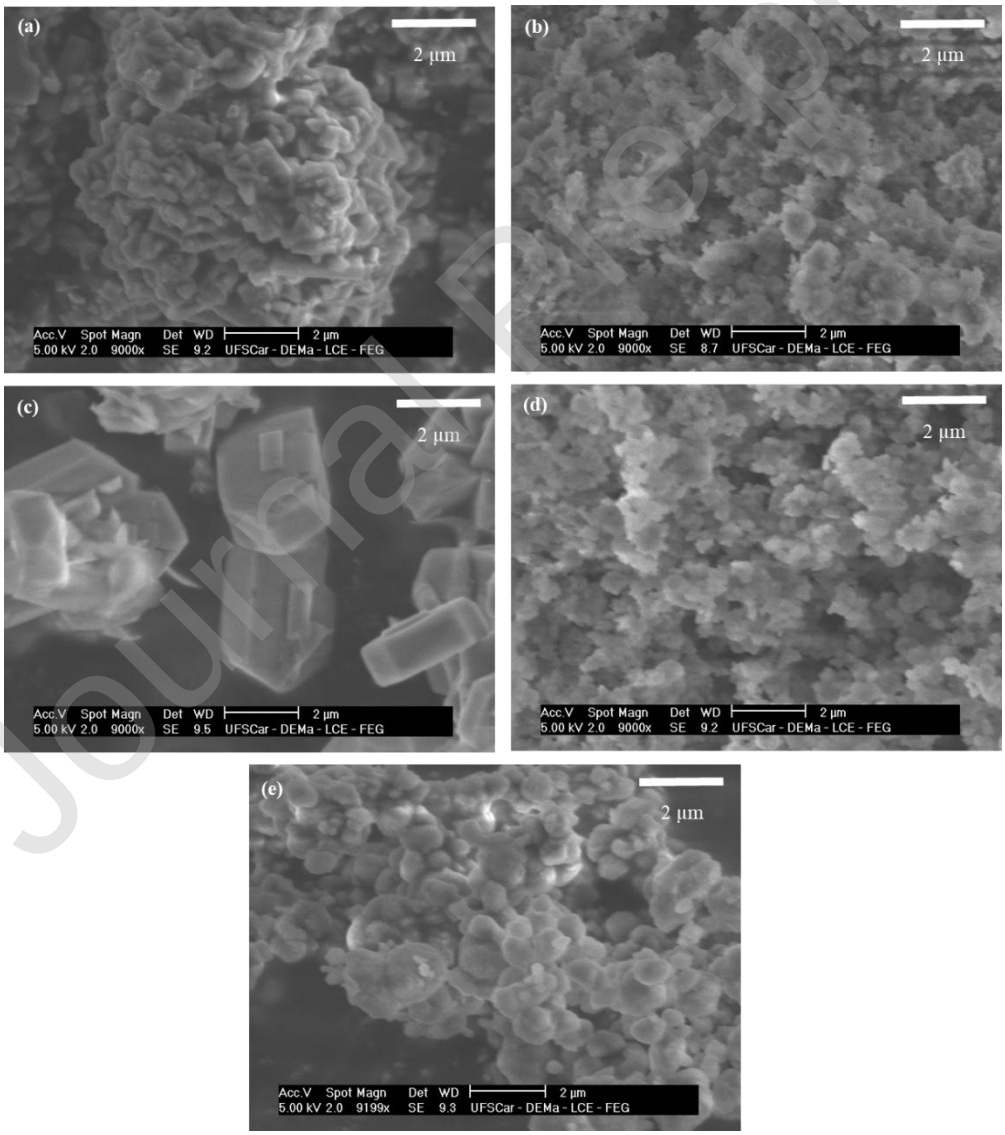

Figure 3. Micrographs of MFI acid zeolites (a) HZ-8, (b) HZ-7, (c) HZ-5, (d) HZ-4 and (e) HZ-3.

The nitrogen physisorption isotherms of the samples are presented in Figure 4, and their textural properties are shown in Table 2. According to IUPAC [19], samples HZ-8, HZ-7, HZ-5, HZ-4, and HZ-3 exhibited type I BET isotherms, possessing high adsorption capacity at low relative pressures, characteristics of materials with micropores.

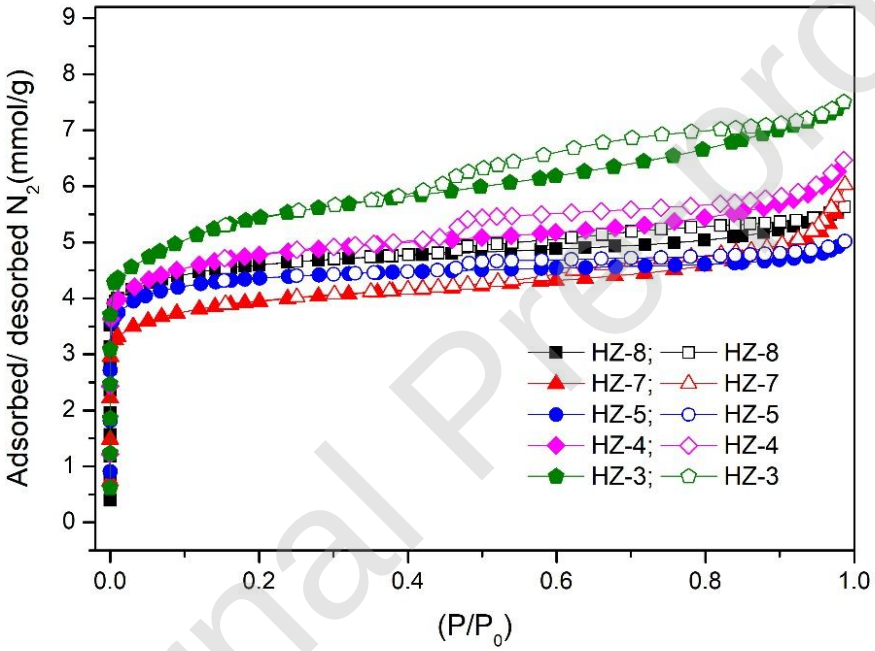

Figure 4. Nitrogen adsorption and desorption physisorption isotherms of samples HZ-8, HZ-7, HZ-5, HZ-4 and HZ-3. Open symbols show desorption.

When applying the t-plot method to these isotherms (Figure 5), it is observed a linearity between the volume and the thickness of nitrogen physisorbed, in the region of P/P_0 between 0.1 and 0.4 (N_2 thickness between 0.36 and 0.49 nm). This allows estimating

the volume of micropores and the external surface of these zeolites, which are shown in Table 2.

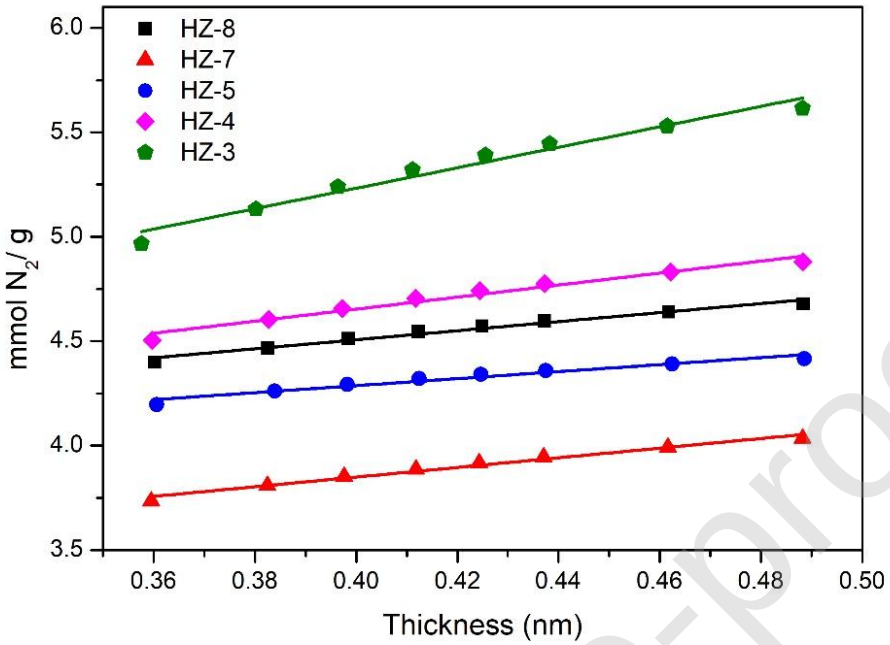

Figure 5. Analysis by t-plot of nitrogen adsorption isotherms of samples HZ-8, HZ-7, HZ-5, HZ-4 and HZ-3.

Analyzing the values of the textural properties of these zeolites, shown in Table 2, it can be observed that there is a tendency for the external area of these materials to increase with the reduction of their aluminum content. For example, the external area (S_{ext}) of the HZ-8 sample is 75.1 m^2/g while HZ-3 was much higher: 169.7 m^2/g. The increase in the external area means that the size of the particles decreases as the aluminum content decreases, which agrees with other authors [18]. The sample HZ-5 is an exception, which, different to the samples manufactured by Zeolyst, has a well-defined habit and much larger particles (Fig. 3c), certainly due to very different synthesis conditions.

Table 2. Textural and catalytic properties of protonic MFI zeolites.

Sample	N_{AS}	V_{micro}[a] (cm^3/g)	S_{ext}[a] (m^2/g)	$dX_A/dt|_{t=0}$ [b] (min^{-1})	TOF_0[c] (min^{-1})
HZ-8	1.3	0.13	75.1	0.082	0.107
HZ-7	1.0	0.10	80.1	0.141	0.229
HZ-5	0.90	0.13	58.1	0.071	0.132
HZ-4	0.67	0.12	99.7	0.210	0.527
HZ-3	0.41	0.11	169.7	0.201	0.829

[a] Determined by the t-plot of the N_2 adsorption isotherms.

[b] Determined by the derivative (for t= 0) of the function adjusted (Eq. 2) to the experimental points (R^2= 0.99).

[c] TOF_0 = turnover frequency at time zero determined by (Eq. 4).

Figure 6 shows the ammonia programmed temperature desorption curves (NH_3 TPD) resulted from the acidic zeolites HZ-8, HZ-7 HZ-5, HZ-4 and HZ-3. The ammonia desorption profiles showed two peaks, the first (A) being around 195-217 ° C and the second (B) between 360-400 ° C. The peak at the lowest temperature is attributed to the desorption of ammonia adsorbed on the ammonium cation [20,21] while the peak at the highest temperature can be explained by the decomposition of the ammonium cation, resulted from adsorption of ammonia to strong acid sites [21].

The ammonia TPD curve of the HZ-5 zeolite has a similar profile to the others, but its maximum desorption peaks A and B are shifted to 20 and 40º C higher temperatures, respectively. To explain this behavior, the micrographs shown in Figure 3c show that this zeolite, unlike the others, has well-formed crystals and of much larger dimensions. Zhao and collaborators [22] found the same effect, of displacement to higher temperatures with increasing particle sizes of their microporous solid. This behavior can be explained by a "labyrinth effect" in which, when dimensions are much larger, the desorbed ammonia molecule takes longer to leave the particle. Consequently, the identification of desorbed ammonia in the gas phase is displaced at higher temperatures.

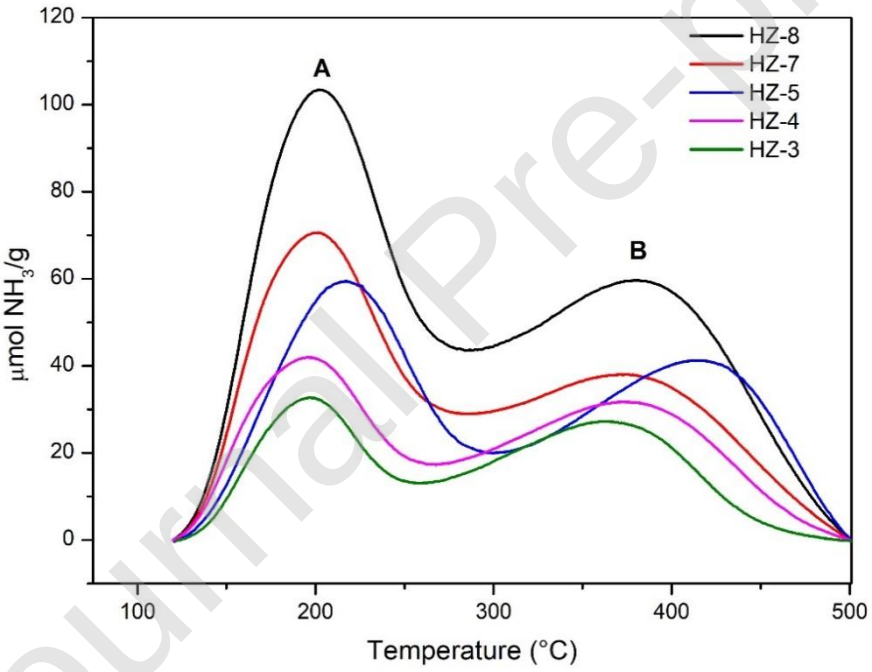

Figure 6. TPD-NH_3 profile of MFI proton zeolites with different framework aluminum content.

Table 3 shows the amount of ammonia desorbed from the zeolites, obtained through the deconvolution of the TPD-NH_3 curves using Gaussian functions (Figure 6), resulting in

adjustments greater than 0.97. The results show that the amount of desorbed ammonia decreases with the reduction of the framework aluminum content in the zeolite, Al_f, shown in Table 1 [15]. This confirms that most aluminum atoms are found in the zeolitic network, thus generating Brønsted acidic sites. In addition, it is observed that the samples HZ-8, HZ-7, HZ-4 and HZ-3 showed NH_3 desorption peak B occurs in the same temperature range, around 360° C (Figure 6), confirming that the acid sites have the same strength, as predicted by Barthomeuf for high Si/Al ratio zeolites [23]. The Table 3 also shows the ratio between the amount of ammonia desorbed at peak A in relation to peak B, with values lower than or equal to 1.0, reinforcing the hypothesis that the first peak is due to the desorption of ammonia that is adsorbed on the cation ammonium, this acting as a Lewis site.

Table 3. Quantification of acidity by NH_3-TPD and the relationship between desorption peaks A and B.

Catalysts	Peak A (°C)	NH_3 peak A[a]	Peak B (°C)	NH_3 peak B[a]	Total NH_3 desorbed[a]	NH_3 peaks A/B ratio
HZ-8	203	695	363	815	1,510	0.85
HZ-7	200	462	358	542	1,004	0.85
HZ-5	217	494	398	494	988	1.0
HZ-4	195	277	362	399	676	0.69
HZ-3	196	193	352	301	494	0.64

Peak A= First peak, Peak B= Second peak.

[a] μmol/g.

3.2.Catalytic Tests

Figure 7 shows the experimental results of the conversions, during two hours of reaction, of acetic acid in isopentyl acetate calculated by Equation 1. The figure also shows the curves adjusted to the experimental data, using Equation 2. Previous works show that the esterification increases with the number of acidic sites [8,11]. However, the results in this Figure 7 show, for example, that the HZ-4 catalyst showed superior catalytic performance to the others, although it has one of the lowest contents of catalytic sites, N_{AS} (Table 1). Similarly, HZ-8 has the highest aluminum content among the other samples but has a very small activity. This suggests that there are other factors that may be influencing catalytic activity.

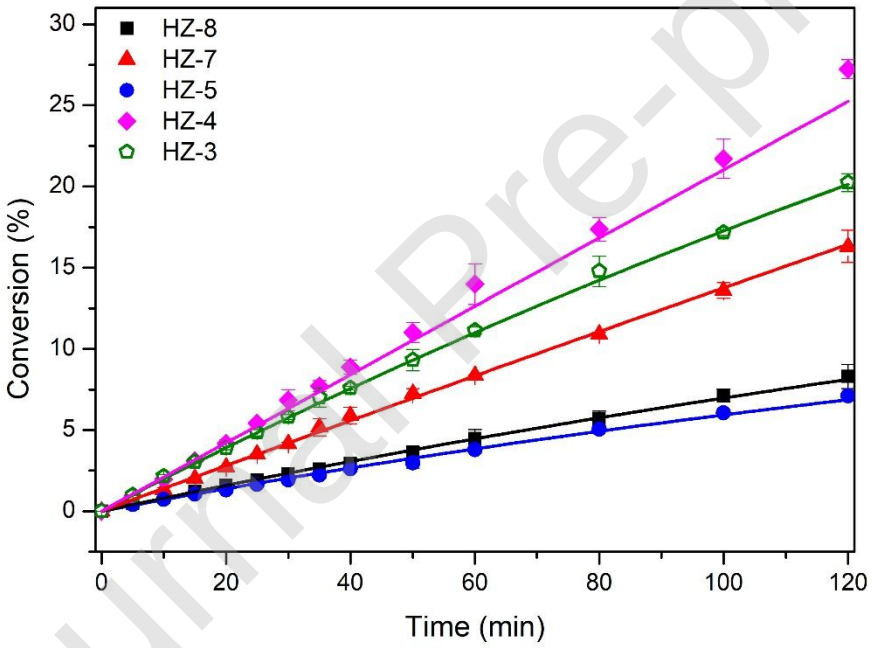

Figure 7. Conversion of acetic acid to isopentyl acetate using proton catalysts with MFI structure.

Analyzing the chemical and catalytic properties of the catalysts presented in Table 2 it is observed that, in general, as the number of catalytic sites (N_{AS}) decreases,

there was an increase in the turnover frequency of the esterification, TOF_0. This result is not expected since, in this range of aluminum content (Table 1), the strength of acidic sites in zeolites is constant [23] and, therefore, TOF_0 should not vary.

Table 2 also shows that as the aluminum content in these zeolites decreased, there is a tendency for their specific external area to increase. Therefore, it can be assumed that, as found by Viswanadham et al [24], the catalytic activity is related to the external surface of the catalysts. This is evident in Figure 8, where there is a pronounced increase in the turnover frequency, TOF_0, with the specific external area of most zeolites. This behavior may be a consequence of limitations of the internal diffusion by some of the reaction components, probably isopentyl alcohol, known as reactant shape-selectivity. Another possibility to explain this behavior could be a consequence of the transition state shape-selectivity. In both types of shape-selectivity, the consequence would be the same, that is, the catalytic action would be occurring preferably on the acid sites present at the outer surface of the particles of these zeolites [25].

This hypothesis is supported by the results presented in Figure 8, in which it is observed that TOF_0 increases with the value of the external area of the zeolites studied. The HZ-5 zeolite does not follow this behavior, but its morphology is completely different from the other samples, as seen in the discussion of the micrograph presented in Figure 3c.

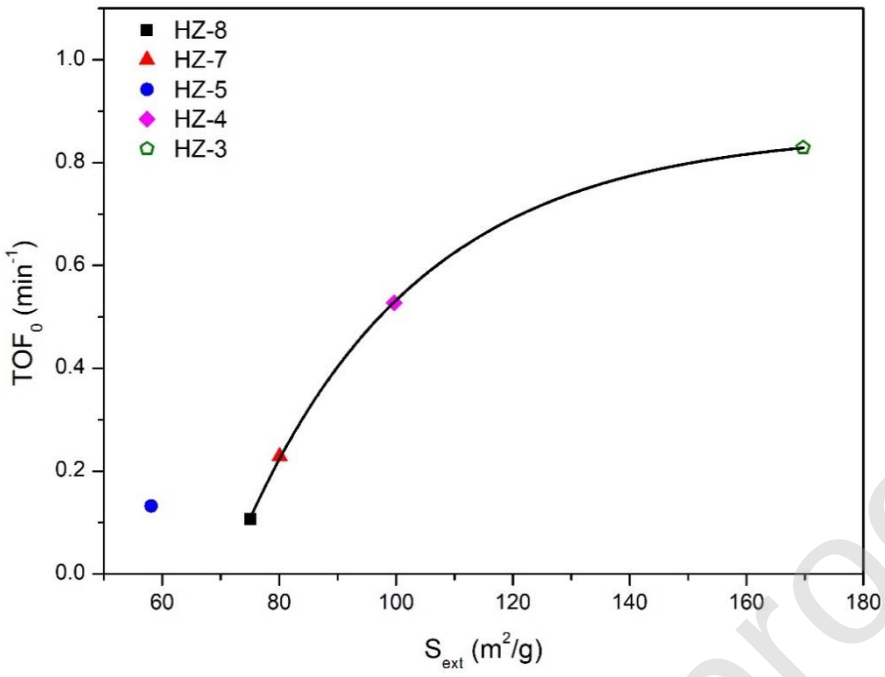

Figure 8. Turnover frequency TOF_0 of the esterification as a function of the external surface area of catalysts HZ-8, HZ-7, HZ-5, HZ-4 and HZ-3.

4. Conclusions

The zeolites with MFI structure with different contents of aluminum are active for esterification of acetic acid with isopentyl alcohol under mild reaction conditions. Contrary to what found by some authors in other zeolites, the increase in aluminum content in the MFI zeolites did not always increase the catalytic activity, estimated by the frequency of molecules transformed per site (TOF_0). According to the results, this unexpected behavior can be attributed to the reduction of the external area of the catalysts with the increase of the aluminum content in the MFI zeolites. This suggests that, due to the diffusional limitation of some component of the reaction in the micropores of the MFI (probably isopentanol or isopentyl acetate), the reaction occurs preferentially on the external surface of the catalyst. Therefore, in defining the catalytic activity for this esterification reaction there are two parameters to be considered: the number of acidic sites and the value of the external surface of the catalyst. According to the results of this work, the main factor that increases the catalytic activity in the formation of isopentyl acetate is the number of acid sites present at the external surface of the catalyst.

CRediT author statement

Maria E. Ribeiro, **Investigation, Analysis, Writing, Review**

Karen N. Franke**, Analysis, Review**

Patrícia M. Lima, **Conceptualization, Review**

Dilson Cardoso, **Conceptualization, Supervision, Review, Funding**

TERM ***DEFINITION***

Conceptualization Ideas; formulation or evolution of overarching research goals and aims

Methodology Development or design of methodology; creation of models

Software Programming, software development; designing computer programs; implementation of the computer code and supporting algorithms; testing of existing code components

Validation Verification, whether as a part of the activity or separate, of the overall replication/ reproducibility of results/experiments and other research outputs

Formal analysis Application of statistical, mathematical, computational, or other formal techniques to analyze or synthesize study data

Investigation Conducting a research and investigation process, specifically performing the experiments, or data/evidence collection

Resources Provision of study materials, reagents, materials, patients, laboratory samples, animals, instrumentation, computing resources, or other analysis tools

Data Curation Management activities to annotate (produce metadata), scrub data and maintain research data (including software code, where it is necessary for interpreting the data itself) for initial use and later reuse

Writing - Original Draft Preparation, creation and/or presentation of the published work, specifically writing the initial draft (including substantive translation)

Review & Editing Preparation, creation and/or presentation of the published work by those from the original research group, specifically critical review, commentary or revision – including pre-or post-publication stages

Visualization Preparation, creation and/or presentation of the published work, specifically visualization/ data presentation

Supervision Oversight and leadership responsibility for the research activity planning and execution, including mentorship external to the core team

Project administration Management and coordination responsibility for the research activity planning and execution

Funding acquisition Acquisition of the financial support for the project leading to this publication

Declaration of interests

The authors declare that they have no known competing financial interests or personal relationships that could have appeared to influence the work reported in this paper.

Acknowledgements

This study was financed by Conselho Nacional de Desenvolvimento Científico e Tecnológico (CNPq) and Coordenação de Aperfeiçoamento de Pessoal de Nível Superior – Brasil (CAPES). The authors thank the Laboratory of Structural Characterization (LCE/DEMa/UFSCar) for the general facilities (SEM-EDS).

5. References

[1] R.N. Vilas Bôas, A.A. Ceron, H.B.S. Bento, H.F. de Castro, Application of an immobilized Rhizopus oryzae lipase to batch and continuous ester synthesis with a mixture of a lauric acid and fusel oil, Biomass and Bioenergy. 119 (2018) 61–68. https://doi.org/10.1016/j.biombioe.2018.09.011.

[2] M.C. Ferreira, A.J.A. Meirelles, E.A.C. Batista, Study of the Fusel Oil Distillation Process, Ind Eng Chem Res. 52 (2013) 2336–2351. https://doi.org/10.1021/ie300665z.

[3] A.G. Patil, S.M. Koolwal, H.D. Butala, Fusel oil: Composition, removal and potential utilization, Int Sugar J. 104 (2002) 51–58.

[4] A. Calam, H. Solmaz, A. Uyumaz, S. Polat, E. Yilmaz, Y. İçingür, Investigation of usability of the fusel oil in a single cylinder spark ignition engine, J Energy Inst. 88 (2015) 258–265. https://doi.org/10.1016/j.joei.2014.09.005.

[5] A. Zaidi, J.L. Gainer, G. Carta, Fatty acid esterification using nylon-immobilized lipase, Biotechnol Bioeng. 48 (1995) 601–605. https://doi.org/10.1002/bit.260480607.

[6] R. Kirdi, N. Ben Akacha, Y. Messaoudi, M. Gargouri, Enhanced synthesis of isoamyl acetate using liquid-gas biphasic system by the transesterification reaction of isoamyl alcohol obtained from fusel oil, Biotechnol Bioprocess Eng. 22 (2017) 413–422. https://doi.org/10.1007/s12257-016-0616-4.

[7] H. Teo, B. Saha, Heterogeneous catalysed esterification of acetic acid with isoamyl alcohol: kinetic studies, J Catal. 228 (2004) 174–182. https://doi.org/10.1016/j.jcat.2004.08.018.

[8] T.A. Peters, N.E. Benes, A. Holmen, J.T.F. Keurentjes, Comparison of commercial solid acid catalysts for the esterification of acetic acid with butanol, Appl Catal A Gen. 297 (2006) 182–188. https://doi.org/10.1016/j.apcata.2005.09.006.

[9] I. Ogino, Y. Suzuki, S.R. Mukai, Esterification of levulinic acid with ethanol catalyzed by sulfonated carbon catalysts: Promotional effects of additional functional groups, Catal Today. 314 (2018) 62–69. https://doi.org/10.1016/j.cattod.2017.10.001.

[10] S.R. Kirumakki, N. Nagaraju, K.V.R. Chary, S. Narayanan, Kinetics of esterification of aromatic carboxylic acids over zeolites Hβ and HZSM5 using dimethyl carbonate, Appl Catal A Gen. 248 (2003) 161–167.

https://doi.org/10.1016/S0926-860X(03)00152-2.

[11] S.R. Kirumakki, N. Nagaraju, K.V.R. Chary, Esterification of alcohols with acetic acid over zeolites Hβ, HY and HZSM5, Appl Catal A Gen. 299 (2006) 185–192. https://doi.org/10.1016/j.apcata.2005.10.033.

[12] J. Bedard, H. Chiang, A. Bhan, Kinetics and mechanism of acetic acid esterification with ethanol on zeolites, J Catal. 290 (2012) 210–219. https://doi.org/10.1016/j.jcat.2012.03.020.

[13] E.O. Akbay, M.R. Altiokka, Kinetics of esterification of acetic acid with n-amyl alcohol in the presence of Amberlyst-36, Appl Catal A Gen. 396 (2011) 14–19. https://doi.org/10.1016/j.apcata.2011.01.013.

[14] V.S. Braga, I.C.L. Barros, F.A.C. Garcia, S.C.L. Dias, J.A. Dias, Esterification of acetic acid with alcohols using supported niobium pentoxide on silica–alumina catalysts, Catal Today. 133–135 (2008) 106–112. https://doi.org/10.1016/j.cattod.2007.12.091.

[15] L. Rodríguez-González, F. Hermes, M. Bertmer, E. Rodríguez-Castellón, A. Jiménez-López, U. Simon, The acid properties of H-ZSM-5 as studied by NH3-TPD and 27Al-MAS-NMR spectroscopy, Appl Catal A Gen. 328 (2007) 174–182. https://doi.org/10.1016/j.apcata.2007.06.003.

[16] M.M.J. Treacy, J.B. Higgins, Collection of Simulated XRD Powder Patterns for Zeolites, Elsevier, 2007. https://doi.org/10.1016/B978-0-444-53067-7.X5470-7.

[17] F.J. Machado, C.M. López, M.A. Centeno, C. Urbina, Template-free synthesis and catalytic behaviour of aluminium-rich MFI-type zeolites, Appl Catal A Gen. 181 (1999) 29–38. https://doi.org/10.1016/S0926-860X(98)00383-4.

[18] L. Shirazi, E. Jamshidi, M.R. Ghasemi, The effect of Si/Al ratio of ZSM-5 zeolite on its morphology, acidity and crystal size, Cryst Res Technol. 43 (2008) 1300–

1306. https://doi.org/10.1002/crat.200800149.

[19] M. Thommes, K. Kaneko, A. V. Neimark, J.P. Olivier, F. Rodriguez-Reinoso, J. Rouquerol, K.S.W. Sing, Physisorption of gases, with special reference to the evaluation of surface area and pore size distribution (IUPAC Technical Report), Pure Appl Chem. 87 (2015) 1051–1069. https://doi.org/10.1515/pac-2014-1117.

[20] N. Katada, H. Igi, J.-H. Kim, Determination of the Acidic Properties of Zeolite by Theoretical Analysis of Temperature-Programmed Desorption of Ammonia Based on Adsorption Equilibrium, J Phys Chem B. 101 (1997) 5969–5977. https://doi.org/10.1021/jp9639152.

[21] M. Niwa, N. Katada, New Method for the Temperature- Programmed Desorption (TPD) of Ammonia Experiment for Characterization of Zeolite Acidity: A Review, Chem Rec. 13 (2013) 432–455. https://doi.org/10.1002/tcr.201300009.

[22] D. Zhao, Y. Zhang, Z. Li, Y. Wang, J. Yu, Synthesis of SAPO-18/34 intergrowth zeolites and their enhanced stability for dimethyl ether to olefins, RSC Adv. 7 (2017) 939–946. https://doi.org/10.1039/C6RA25080G.

[23] D. Barthomeuf, Zeolite acidity dependence on structure and chemical environment. Correlations with catalysis, Mater Chem Phys. 17 (1987) 49–71. https://doi.org/10.1016/0254-0584(87)90048-4.

[24] N. Viswanadham, R. Kamble, M. Singh, M. Kumar, G. Murali Dhar, Catalytic properties of nano-sized ZSM-5 aggregates, Catal Today. 141 (2009) 182–186. https://doi.org/10.1016/j.cattod.2008.03.026.

[25] S.M. Csicsery, Shape-selective catalysis in zeolites, Zeolites. 4 (1984) 202–213. https://doi.org/10.1016/0144-2449(84)90024-1.